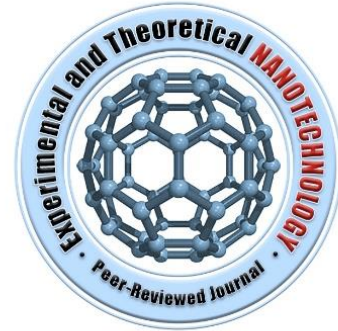# Theoretical investigation of slow-light VCSEL amplifier

Ahmed M. A. Hassan[1,2,], Moustafa Ahmed[3], M. Nakahama[1], Fumio Koyama[1]*

[1]Laboratory for Future Interdisciplinary Research on
Science and Technology, Tokyo Institute of Technology, Yokohama 226-8503, Japan.
[2]Department of Physics, Faculty of Science, Al-Azhar University, Assiut Branch, Egypt.
[3]Department of Physics, Faculty of Science, Minia University, 61519 Minia, Egypt.
*) Email: ah.hassan84@gmail.com

We present numerical analysis of a slow-light vertical-cavity surface-emitting laser (VCSEL) amplifier basing on a travelling wave model. The model takes into account two oscillating modes; the vertical lasing mode and a slow light mode. We describe the amplification of the slow light mode through the amplifier when it is biased above the threshold level of the vertical lasing mode. The output power is investigated at different bias currents and lengths of the amplifier. The numerical results ascertain the possibility to obtain high gain more than 22 dB for amplifier length of 1 mm.

1. INTRODUCTION

There is always an interest in boosting the performance of VCSEL. Due to its superiority, VCSEL is an important optical source for wide range of applications. Compared to other semiconductor lasers, VCSELs are low-cost, easy to fabricate in two-dimensional arrays, wafer-level testing low threshold current, low power consumption, low diversions and high beam quality [1].

Moreover, VCSEL supports single longitudinal mode because of the short length cavity in-between two highly reflective distributed Bragg reflector (DBR) mirrors. Also, to confine the output of VCSEL into single transverse mode, the oxidization confinement aperture is usually

reduced to 2-3 μm [2]. This small cavity size leads to low output power not exceeding few milli-watts [3]. High power VCSEL is still a big challenge, especially for applications like as free space communications [4], material welding and processing [5], and self-driving cars based on light detection and ranging (LiDAR) systems [6].

Many different approaches to scale-up the output power of VCSELs have been proposed. Combing a large number of VCSELs in 2-dimentional arrays can push the power to Watt-regimes. 10 W output of VCSEL arrays were reported in [7], with conversion efficiency more than 20%. The total output power of array constitutes a single lobe was obtained with small divergence in comparison to high power edge emitting laser bars, with many significant contributions having been done to improve the beam quality of the array's main lobe [8]. Distinctive 6x6 arrays with stable single lobe in the far field were obtained by weak coupling of single mode VCSEL array [9]. A. Pruijmboom and *et.al*. [9, 10] demonstrated high power VCSEL arrays in the range of kilo-Watt levels for thermal treatment and other industrial application [9,10]. VCSELs with a large aperture can provide high power but with a low beam quality [11]. In phase coherent coupling, beam steering and beam shaping are still needed to more improvement toward enhancing the VCSEL's power for industrial applications [9].

Recently, Koyama's group proposed a new approach to boost the output power of VCSEL [12]. This scheme is based on slowing down light in a Bragg reflector waveguide [13]. Controlling the light velocity in the waveguide is an attractive phenomenon that improves light-matter interactions [14]. Many novel devices and new VCSEL functionalities are proposed basing on slow light waveguides such as high speed modulators [1, 6], transverse coupled cavity VCSELs [15], beam scanners [1], switches [6] and semiconductor optical amplifiers [12]. Reducing the light velocity in the Bragg reflection waveguide may be considered as a result of its zigzag-like propagation, when the optical wave experiences consecutive reflections from the Bragg mirrors as shown in Fig. 1(a) [12]. This waveguide is aimed to guide light in the core with refractive index lower than the surrounding cladding refractive index [16,17]. The group velocity v_{gs} is defined as $\frac{\partial \omega}{\partial \beta}$, where ω is angular wave length of guided light. The propagation constant for Bragg-reflectors is determined by the relationship [18]:

$$\beta = 2\pi n \left(\frac{1}{\lambda^2} - \frac{1}{\lambda_c^2} \right)^{1/2} \tag{1}$$
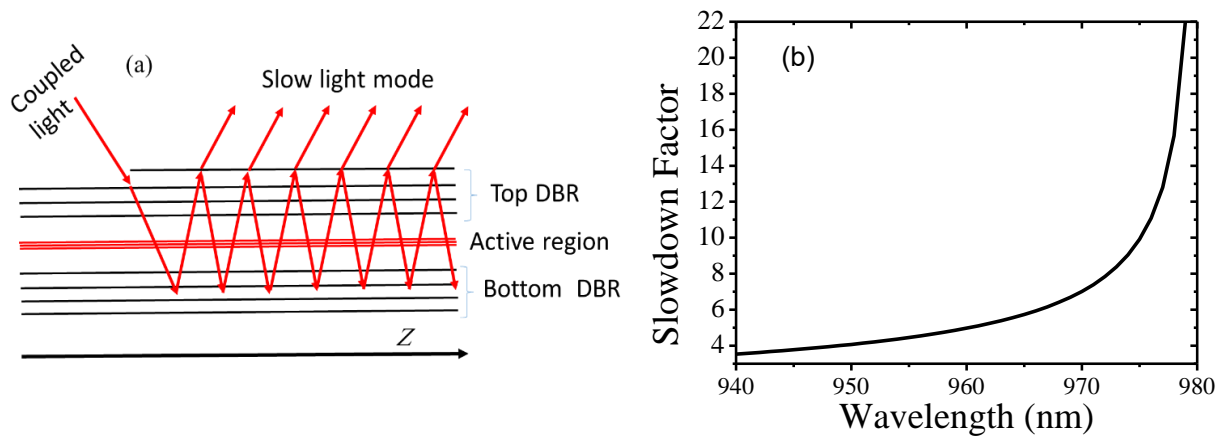
Figure 1 (a) Bragg-reflector waveguide, (b) slowing down factor vs wavelength of propagation light in Bragg-reflector waveguide

Figure 1(b) shows the slow down factor versus wavelength. Close to the cut-off wavelength λ_c of the Bragg waveguide, the propagation constant β is highly dispersive [19]. In this case, the propagation constant is dramatically decreased and hence the group velocity is also reduced by factor f called slow-down factor and defined as:

$$f = \frac{v}{v_{gs}} = \frac{n_g}{n} \tag{2}$$

From Eq's. (1) and (2), the group velocity vgs can be seriously shrink when the light is tuned close to the cut-off wavelength of the Bragg-reflector waveguide. DBRs themselves serve as mirrors with high reflectivity to confine the optical field in the optical cavity and VCSEL gain medium [1]. Because of structure similarity between the VCSEL and Bragg-reflector waveguide, it's easy to integrate them together and create new functionalities [6].

In this paper, we introduce numerical analysis of a novel scheme of slow-light VCSEL amplifier to improve output power of VCSELs to the Watt-class. The VCSEL is assumed biased above the threshold level. Both the rate equation and travelling wave models are used for describing a lasing mode and a slow light mode through the VCSEL cavity. For simplicity, we used single lasing mode rate equations. Although a long cavity supports many transvers

vertical modes, using single mode rate equations is still accurate to a great extent because all of these modes are assumed to be uniform. We optimize the amplifier length, current, top mirror reflectivity and input power saturation for the purpose of high power VCSEL applications.

2. THEORETICAL MODEL AND CALCULATIONS

The proposed slow-light VCSEL amplifier has the same structure of a conventional VCSEL [12]. Figure 2 shows the structure of this VCSEL amplifier. The active region and an oxidization confinement layer are sandwiched by two DBR mirrors. A slow-light mode is then excited along the waveguide. This slow light propagates with group velocity v_{gs} and the top mirror reflectivity is designed to allow for portion of light to go outside the cavity as radiation loss. Because, the top-mirror reflectivity depends on the number of DBR pairs, it's important to optimize the number of DBR layers to get enough radiation output light. High loss from travel waves can be compensated by current injection to the active region. To get more output power, the length of amplifier and injection current should be increased. By raising current above the threshold current, the light intensity of the slow light mode becomes more uniform along the amplifier and the beam divergence get narrower. As a result of output uniformity along the cavity, the output power is directly proportional to the length of amplifier [12].

Our analysis of the VCSEL amplifier is based on a travel-wave equation of the slow light mode in the VCSEL gain medium. In addition to the slow light mode, there is a vertical lasing mode which has a zero group velocity in the horizontal direction. The lasing mode gain and loss are almost the same for the slow light mode, which propagates in the lateral direction. We consider the forward component only for the slow light that moves in the positive z-direction. The rate equations are then written as:

$$\frac{dS_l}{dt} = v_g(\Gamma_l g - \alpha_i - \alpha_m)S_l + \Gamma_l \acute{R}_{sp}$$

(3)

$$\frac{1}{v_{gs}}\frac{dS}{dt} + \frac{dS}{dz} = f(\Gamma g - \alpha_i - \alpha_r)S \tag{4}$$

$$\frac{dN}{dt} = \frac{\eta I}{qV} - (R_{sp} + R_N) - v_g g S_l - f v_{gs} g_s S \tag{5}$$

where S_l, S, v_g and v_{gs} are photon densities and group velocities for the vertical lasing mode and slow light mode, respectively. R_{sp} and R_N represent the spontaneous and non-radiative

recombination rates. η is the injection efficiency or internal quantum efficiency, I is injection current, q is elementary charge and V is volume of active region α_m is the mirror loss whereas α_i is the internal cavity loss. α_r is slow light radiation loss which constitutes the output power of the slow light mode and its value is approximately equal to α_m. A logarithmic expression is simply used for gain $g = g_0 \log\left(\frac{N}{N_{tr}}\right)$, where g_0 is the gain coefficient and N_{tr} is the transparent carrier density [20].
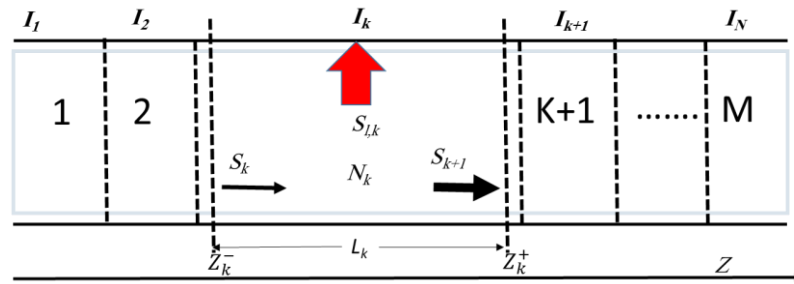
Figure 2 Schematic diagram of the VCSEL amplifier divided into K sections.

These rate equations are complicated and difficult to be solved analytically. The numerical solution is obtained by dividing the amplifier into small sections as seen in Fig. 2. The injection current is assumed uniformly distribution along the cavity. Every section work as a small amplifier and the position dependency is cancelled.

2.1 Steady –state solutions

At steady state, time derivative is vanished. So, by integrating Eq. (4), the solution becomes:

$$S_{out}(k) = S_{in}(k)\exp\left[f\left(\Gamma g_0 \log\left(\frac{N}{N_{tr}}\right) - \alpha\right)z\right] \quad , k \text{ is section number} \tag{6}$$

where S_{out} is the photon density traveling from one section to the other inside the cavity. The boundary conditions for the amplifier sections are:

$$S_{in}(k) = S_{out}(k-1), \tag{7}$$

$$S_{in}(1) = S_{input} \tag{8}$$

and $S_{input} = \frac{\Gamma P_{in}}{w L_a v_{gs} E_s}$. $\tag{9}$

where $E_s = \frac{hC}{\lambda_s}$ with λ_s being the wavelength of the slow light mode. In and out in these equations refer to the input and output of the section. The output radiation light will introduced below. Generally, using average of photon density [21, 22] will increase the accuracy of calculation especially when the length is large enough to reduce the time of calculations. The average value of the photon density in a section with length L_z.is

$$S_{av}(k) = \frac{1}{L_z} \int_{L-L_z}^{L+L_z} S_{in}(k) \exp\left[f\left(\Gamma g_0 \log\left(\frac{N}{N_{tr}} \right) - \alpha \right) z \right] dz \tag{10}$$

$$S_{av}(k) = \frac{\exp\left[f\left(\Gamma g_0 \log\left(\frac{N}{N_{tr}} \right) - \alpha \right) L_z \right] - 1}{f\left(\Gamma g_0 \log\left(\frac{N}{N_{tr}} \right) - \alpha \right) L_z} S_{in}(k) \tag{11}$$

By substitution for S_l and S_{av} from Eqs. (3) and (11) into Eq. (5), we get:

$$\frac{\eta_i I_k}{q V_k} - \left(A N_k + B N_k^2 \right) - g_0 \log\left(\frac{N_k}{N_{tr}} \right) \frac{\Gamma \beta B N_k^2}{\left(\alpha - \Gamma g_0 \log\left(\frac{N_k}{N_{tr}} \right) \right)}$$

$$- f v_{gs} g_0 \log\left(\frac{N_k}{N_{tr}} \right) \frac{\exp\left[f\left(\Gamma g_0 \log\left(\frac{N_k}{N_{tr}} \right) - \alpha \right) L_z \right] - 1}{f\left(\Gamma g_0 \log\left(\frac{N_k}{N_{tr}} \right) - \alpha \right) L_z} S_{in}(k) = 0 \tag{12}$$

Equation (12) is nonlinear in N_k and is solved numerically; hence the photon densities and outputs for the lasing and slow light modes can be determined in all sections. For the slow light mode, the output power is given by:

$$P_{out} = f \alpha_m \left[\frac{\exp\left[f\left(\Gamma g_0 \log\left(\frac{N}{N_{tr}} \right) - \alpha \right) L_z \right] - 1}{f\left(\Gamma g_0 \log\left(\frac{N}{N_{tr}} \right) - \alpha \right) L_z} S_{in}(k) \right] V_p v_{gs} E_s \tag{13}$$

when $\Gamma g - \alpha$ approaches to zero above threshold, and hence the term $\frac{\exp\left[f\left(\Gamma g_0 \log\left(\frac{N}{N_{tr}} \right) - \alpha \right) L_z \right] - 1}{f\left(\Gamma g_0 \log\left(\frac{N}{N_{tr}} \right) - \alpha \right) L_z}$

approaches unity. So, the output power becomes

$$P_{out} = f \alpha_r [S_{in}(k)] V_p v_{gs} E_s \tag{14}$$

$$P_{out} = \alpha_m S_l V_p v_g E_v \tag{15}$$

## 3. RESULTS AND DISCUSSION

Rate equations (3) – (5) are solved in the steady state for a wide range of parameters, including input power, injection current and length of amplifier. The section length decides the accuracy

of calculations. Smaller section length corresponds to means longer time but more accuracy of calculations. We use the length of section ranging from 5 to 20 µm. The calculation accuracy does not noticeably change over this range.

A. *Uniform output power along amplifier*

When VCSEL amplifier is biased above threshold, the output power will be uniformly distributed along the amplifier. To investigate the uniformity of the output power, we first calculate the photon density along the amplifier at different currents. Figure 3 shows the dependency of the photon density of the lasing mode along the amplifier on the injection current. As shown in the figure, at currents below threshold, the loss is higher than gain. As result of high loss, the slow light is decreased dramatically and the effective radiation length is limited to few microns. Above the threshold level, stimulated emission compensates the total loss (internal and radiation losses) and the radiation length increases by increasing the current.
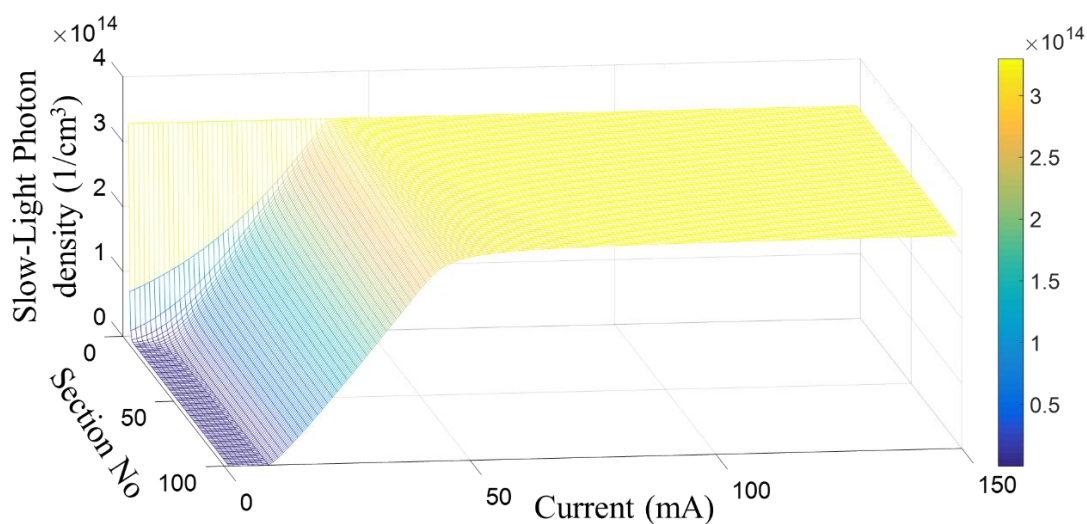

Figure 3 show density of photon radiation along VCSEL amplifier with length = 1mm and input power=0.5 mW. Amplifier divide into 50 section.

As inferred from the steady-state solution of the rate equation, the gain is not equal loss exactly at and the above threshold. By increasing the injection current, gain approaches to the loss and the output of the lasing mode is growing up linearly. At same time, the gain factor of the slow

light mode approaches unity as we can see from equations (13). This mean that by increasing the current above threshold, one can extend the length of the amplifier even several centimeters with uniform output power along the amplifier.

### B.   *L-I characteristics of lasing mode and slow light mode*

It's important to investigate the light-current (L-I) characteristics and clarify the growing and/or suppression of the slow light and lasing modes. The input power Pin increases from zero to 1 mW, and the amplifier length is set to 1 mm. Figure 4 shows that the increase in the input power coupled to the slow light mode leads to an increase in the threshold current of the lasing mode. This is because of increasing slow light photons in the cavity, which will combine and deplete charge carriers by stimulated emission. Hence, the carrier density goes down to a level lower than the threshold carrier density. In this case, extra current is needed to reach again to the threshold level. Figure 4(a) shows that the threshold current with no input power is equal to 30 mA, while for input power Pin = 0.5 mW, the threshold current is 90 mA. Figure. 4(b) shows the corresponding output power of slow light. As shown in the figure, once the lasing mode reaches the threshold the slow light mode saturates. Increasing the input power requires high current to show this saturate.
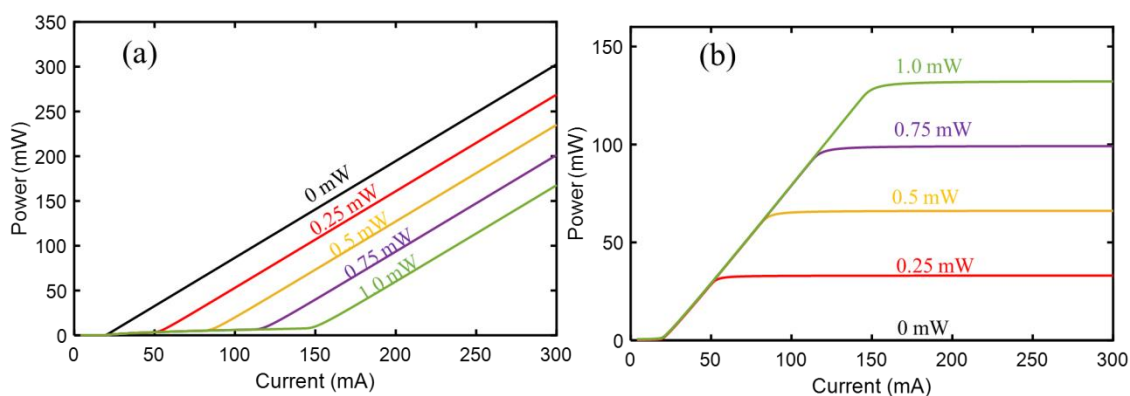
Figure.4 output of lasing mode (a) and slow light mode (b) for amplifier length = 1mm and input power range from Pin = 0 up to 1.0 mW.

In Fig. 5, we analyze suppression of the lasing mode at current I = 10Ith for the amplifier of length 1 mm. When the lasing mode is completely turned off, the output power of the slow light mode will saturate at almost 400 mW. Figure 5 shows the switching behavior of the

vertical lasing mode as a function of the input power coupled to the slow light mode. 100 uniform lasing modes are considered in the calculations of this figure.
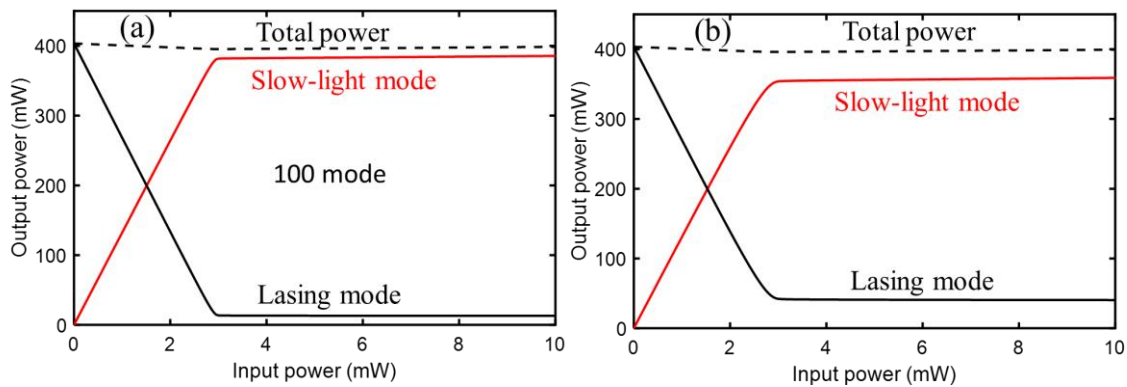
Figure 5 Switching of the lasing mode as function of the input power coupled to slow light mode: (a) 100 lasing modes, and (b) 500 lasing modes.

The origin of these modes is the amplified spontaneous emission (ASE) which has a chance to lase. When the carrier density approaches the threshold value, the spontaneous emission modes prohibit the slow light mode to reach the intensity of the lasing mode when there is no input power. In Fig. 5(b), the number of modes is increased to 500. The output power of the slow light mode is decreased below the total power or the lasing power. The carriers consumed by ASE are one limitation to reach the maximum high power of the amplifier.
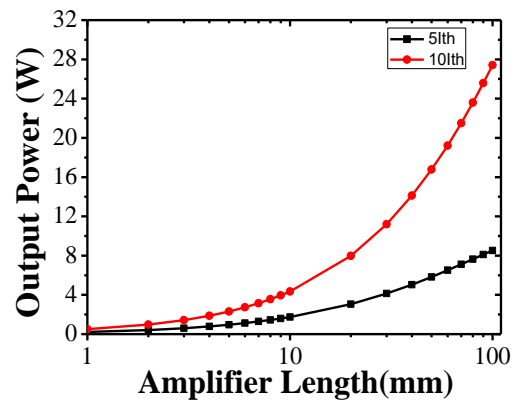
C. Gain of VCSEL amplifier

To evaluate the amplification performance of the amplifier, we calculate the optical gain from the relation between the output power and input power coupled to the slow light mode. The gain in decibel is defined as:

$$Gain\ (dB) = 10log\ \left(\frac{P_{out}}{P_{in}}\right) \tag{16}$$

The gain is clamped at a fixed value as long as lasing mode is turned on. Due to suppression of the lasing mode, any increase in the input power will lead to drop of the gain. The maximum gain for 1 mm-length amplifier is 23 dB. Figure 6(a) shows the gain curve for the 1 mm-amplifier at I = 2Ith, 4Ith and 6Ith. This value of gain is much more than the value obtained when amplifier is biased under threshold [23].
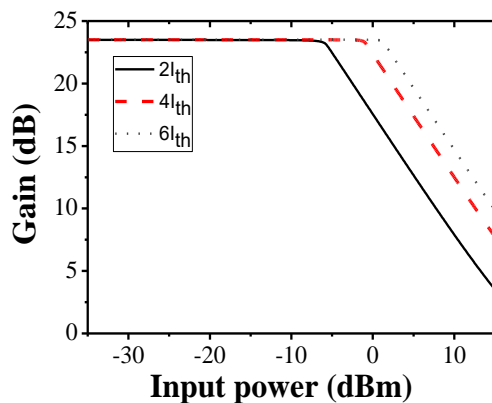
Figure. 6. Gain of 1mm VCSEL amplifier as function of input power.

Figure. 7. Saturation of output power as function of amplifier length at 5 and 10 I_{th} .

D. Elongated VCSEL amplifier

To increase the output power to over than 20 W, the length of the amplifier should be extended up to more than 5 cm. Figure 7 shows the saturated output power for amplifier lengths in the range from 1 to 100 mm. The 29 W output power can be obtained for a length of 10 cm at current equal 10 I_{th}.

4. CONCLUSIONS

We developed a travel wave model to describe characteristics of a slow-light VCSEL amplifier. The model introduced detailed description of the slow light mode amplification when the amplifier is biased above threshold. Influences of the operation critical parameters, including the input power, length of amplifier and bias current were investigated. Our calculation took into account two modes; a vertical lasing mode and a slow light mode. The numerical results showed the possibility to obtain Watt-class output power by extending the length of the

amplifier to several centimeters. This device is promising for high power applications, such as LiDAR systems and beam scanners.

References

[1] F. Koyama, J. Lightw. Technol. 24, 4502–4513 (2006).

[2] Nikolay N. Ledentsov, James A. Lott, Jörg-R. Kropp, Vitaly A. Shchukin, and et.al, Proc. SPIE 8276, (2012).

[3] M. Grabherr, M. Miller, D. Wiedenmann, R. Jäger and R. King, Proc. SPIE 6484 (2007).

[4] M. Yoshikawa, A. Murakami, J. Sakurai, H. Nakayama and T. Nakamura, Proceedings Electronic Components and Technology, 2005. ECTC '05., 2, 1353-1358, (2005).

[5] D. Zhou, J. Seurin, G. Xu, P. Zhao, B. Xu, T. Chen, R. van Leeuwen, J. Matheussen, Q. Wang and C. Ghosh, Proc, of SPIE, 9381 93810B-1 (2015).

[6] F. Koyama and X. Gu, IEEE J. Sel. Topics in Quantu. Electron., 19, 1701510-1701510, (2013).

[7] M. Miller, M. Grabherr, R. Jager and K. J. Ebeling, IEEE J. Photon. Techn. Letters, 13, 173-175, (2001).

[8] J. W. Shi, K. L. Chi, J. H. Chang, Z. R. Wei, J. W. Jiang and Y. J. Yang, IEEE J. Photon., 5, 1502508-1502508, (2013).

[9] A. Pruijmboom, R. Apetz, R. Conrads, C. Deppe, G. Derra, S. Gronenborn, J. S. Kolb, H. Moench, F. Ogiewa, P. Pekarski, et al., J. Laser Appl., 28, 032005,(2016).

[10] H. Moench, R. Conrads, C. Deppe, G. Derra, S. Gronenborn, Xi Gu, G. Heusler, J. Kolb, et.al, Proc. SPIE 9348, (2015).

[11] Y-Qin Hao, Y. Luo, Y. Feng,1 Chang-Ling Yan,et al., J. Appl. Optic.,50, 1034-1037, (2011).

[12] M. Nakahama, X. Gu, A. Matsutani, T. Sakaguchi and F. Koyama, Conference on Lasers and Electro-Optics (CLEO), San Jose, CA, 1-2, (2016).

[13] G. Hirano and F. Koyama, LEOS 2007 - IEEE Lasers and Electro-Optics Society Annual Meeting Conference Proceedings, Lake Buena Vista, FL, 86-87, (2007).

[14] T. Baba, Nature Photonics, 2, 465 – 473, (2008).

[15] H. R. Ibrahim, M. Ahmed and F. Koyama, 20th Microoptics Conference (MOC), Fukuoka, 1-2, (2015).

[16] A. Y. Cho, A. Yariv, and P. Yeh, Appl. Phys. Lett., 30, 47,1 (1977).

[17] P. Yeh, A. Yariv, and Emanuel Marom, J. Opt. Soc. Am, 68, 1196-1201, (1978).

[18] Bahaa E. A. Saleh, Malvin Carl Teich, Fundamentals of Photonics, 2nd Edition, Wiley (2007).

[19] Yasuki Sakurai and Fumio Koyama, Jpn. J. Appl. Phys. 43 5828, (2004).

[20] L. A. Coldren, S. W. Corzine, and M. L. Mashanovitch, Diode Lasers and Photonic Integrated Circuits, 2nd Edition., John Wiley & Sons, Inc.

[21] M. J. Adams, J. V. Collins, and I. D. Henning, Proc. IEE Optoelectron., 132, 58–63, (1985).

[22] T. Durhuus, B. Mikkelsen, and K. E. Stubkjaer, J. Lightw. Technol., 10, 1056–1065, (1992).

[23] T. Shimada, A. Matsutani, and F. Koyama, Appl. Phys. Lett. 6, 2102, (2013).